21.08.2021.

Treatment of disorder effects in X-ray absorption spectra by reverse Monte Carlo simulations: $CuMoO_4$ case

Inga Pudza, Alexei Kuzmin

Institute of Solid State Physics, University of Latvia

E-mail: inga.pudza@cfi.lu.lv

LATVIJAS UNIVERSITĀTES
CIETVIELU FIZIKAS INSTITŪTS
INSTITUTE OF SOLID STATE PHYSICS
UNIVERSITY OF LATVIA

EXAFS Lab

http://www.dragon.lv/exafs

MOTIVATION I

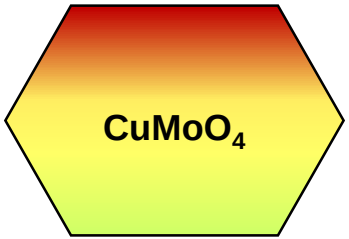

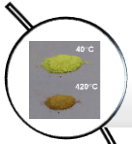

Thermochromic

T. G. Steiner, et al., J. Anal. Chem. 370, 731 (2001);
M. Gaudon, et al., Inorg. Chem. 46 (2007) 10200–10207;
I. Yanase, et al., Ceram. Int. 39 (2013) 2059–2064;
L. Robertson, et al., J. of Materials Chem. C 3 (2015) 2918-2924;
N. Joseph, et al. Applied Materials & Interfaces 12.1 (2020) 1046-1053;

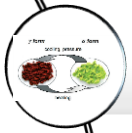

Piezochromic

M. Wiesmann, et al., J. Solid State Chem. 132 (1997) 88-97;
F. Rodríguez, et al., Phys. Rev. B 61 (2000) 16497;
M. Gaudon et al., Adv.Mater.19 (2007) 3517;
L. Robertson, et al., J. of Materials Chem. C 3 (2015) 2918-2924;

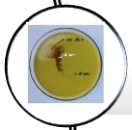

Halochromic (pH)

K. S. Makarevich, et al., Inorg. Mater. 46 (2010) 1359-1364;

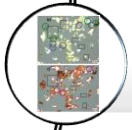

Thermosalient effect

L. Robertson, et al., J. of Materials Chem. C 3 (2015) 2918-2924;

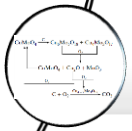

Catalytic

T.K. Ghorai et al., Mater. Res. Bull. 43 (2008) 1770;
K. S. Makarevich, et al., Inorg. Mater. 46 (2010) 1359;
P. Chigrin, et al., Kinetics and Catalysis 54 (2013) 76-80;

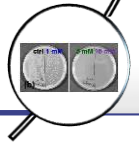

Antibacterial

D. Tanasic, et al., Biointerphases 12 (2017) 05G607.

MOTIVATION II

Thermochromic properties

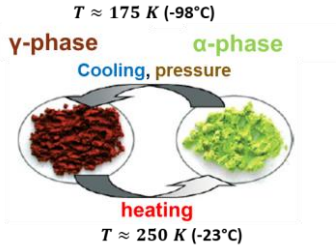

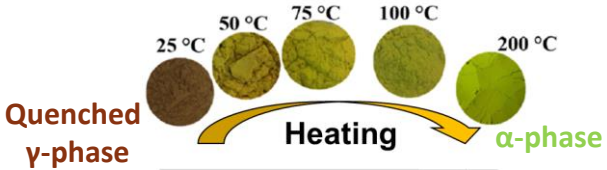

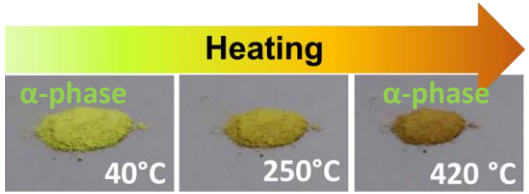

T. G. Steiner, et al., J. Anal. Chem. 370 (2001) 731.
M. Gaudon, et al., Inorg. Chem. 46 (2007) 10200-10207.
I. Yanase, et al., Ceram. Int. 39 (2013) 2059-2064.
L. Robertson, et al., J. of Materials Chem. C 3 (2015) 2918-2924.
N. Joseph, et al. Applied Materials & Interfaces 12.1 (2020) 1046-1053.

Applications

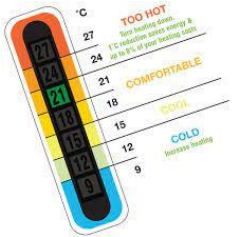

https://www.hallcrest.com/
https://colourchanging.co.uk/

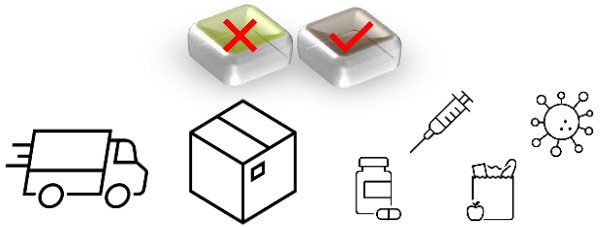

$CuMoO_4$

At low temperatures

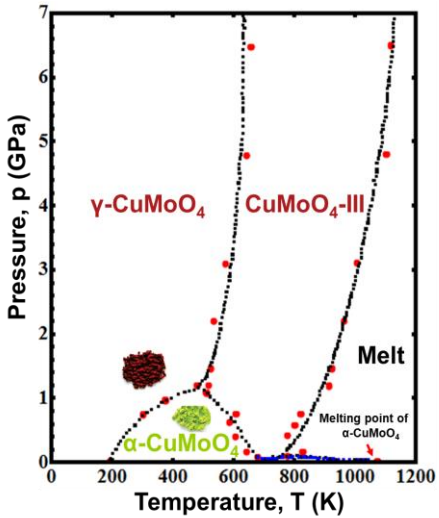

M. Wiesmann, et al., J. Solid State Chem. 132 (1997) 88.

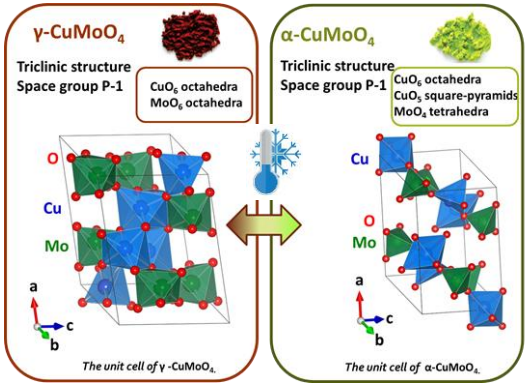

$\Delta V \approx 12 - 13\%$

Unit cell: 36 atoms
- 2 x(Cu1+Cu2+Cu3)
- 2 x(Mo1+Mo2+Mo3)
- 2 x12 xO

Hysteresis

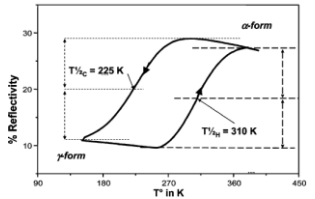

Figure 6. Evolution of the integrated reflectivity percentage in the green zone (500−550 nm) of $CuMo_{0.9}W_{0.1}O_4$ compound with temperature.

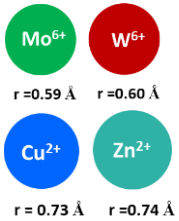

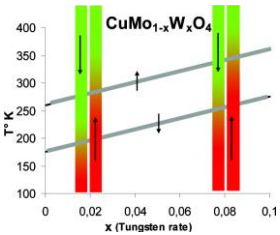

M. Gaudon, et al., Inorg. Chem. 46 (2007) 10200-10207.
T. Ito, et al., Chem. of Mat., 21 (2009) 3376-3379.
X. Wu, et al., Mater. Res. Express 7 (2020) 016309.

$CuMoO_4$

At high temperatures

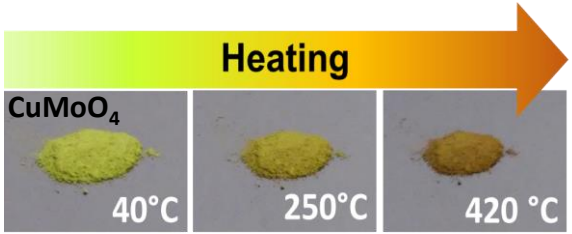

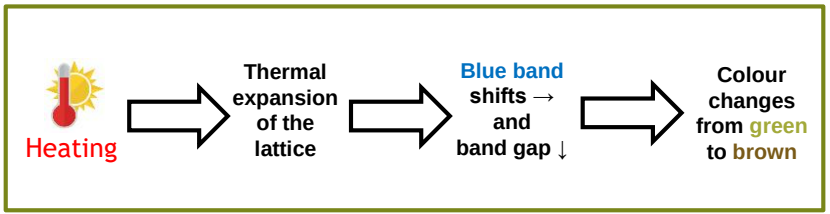

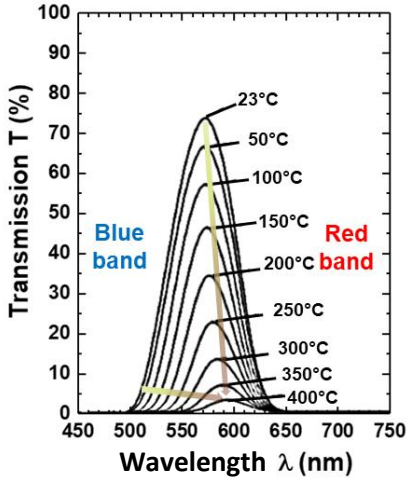

Blue band
$O^{2-} \rightarrow Cu^{2+}$
$O^{2-} \rightarrow Mo^{6+}$
$Cu^{2+} \rightarrow Mo^{6+}$
charge transfer processes

Red band
Cu^{2+} d-d transitions
Cu^{2+} $3d^9 \rightarrow 4p$

T. G. Steiner, et al., J. Anal. Chem. 370 (2001) 731.
F. Rodríguez, et al., Phys. Rev. B 61 (2000) 16497.
M. Gaudon, et al., Inorg. Chem. 46 (2007) 10200-10207.
S. Dey, et al., Inorg. Chem. 53 (2014) 4394-4399.

$CuMoO_4$ AT LOW TEMPERATURES - XANES

PETRA III beamline P65

1s(Mo)->4d(Mo)+2p(O)

Experiment

Theory

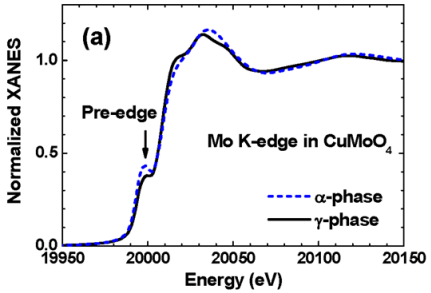

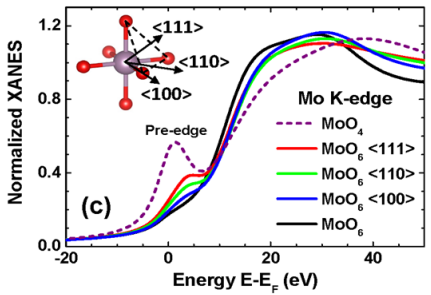

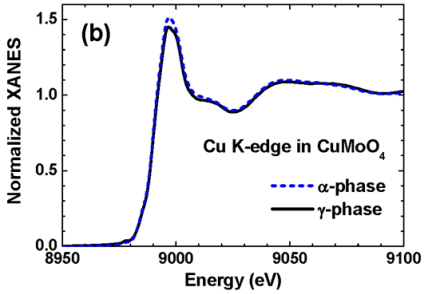

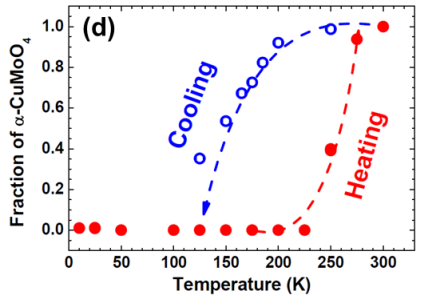

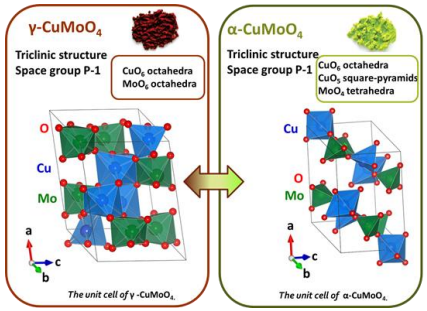

$CuMoO_4$	Phase transition T
α -> γ	200-120K
γ -> α	230-280K

I. Jonane, A. Cintins, A. Kalinko, R. Chernikov, A. Kuzmin, *Low Temp. Phys.* 44 (2018) 568-572.

Linear combination analysis of Mo K-edge XANES allows one to reconstruct the hysteresis curve that describes the phase transition.

$CuMoO_4$ AT LOW TEMPERATURES - EXAFS

Experiment

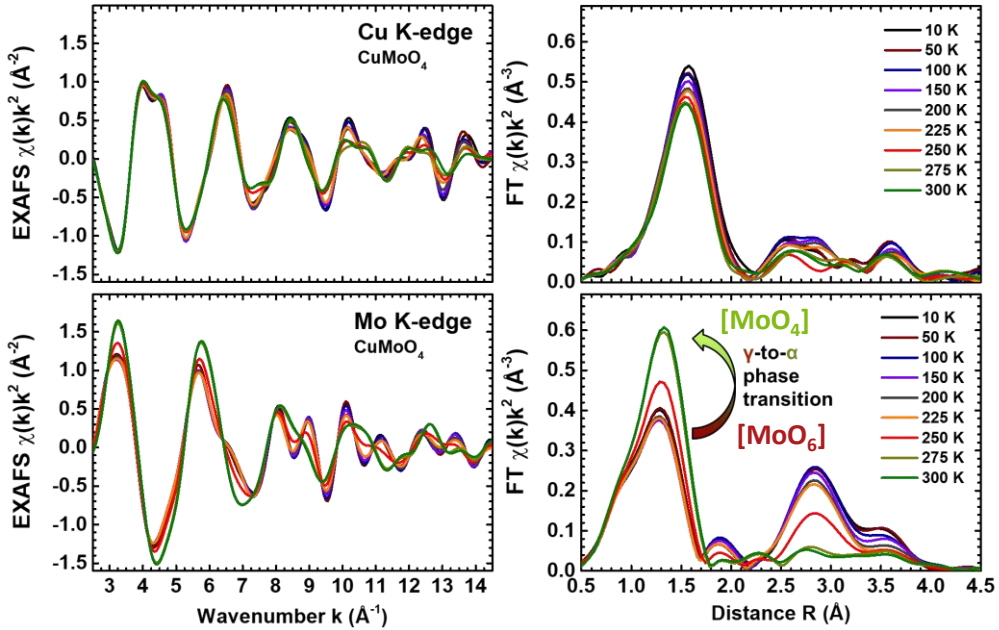

Experimental EXAFS spectra show significant differences between α un γ phases.

EXAFS DATA ANALYSIS

using regularization-based technique

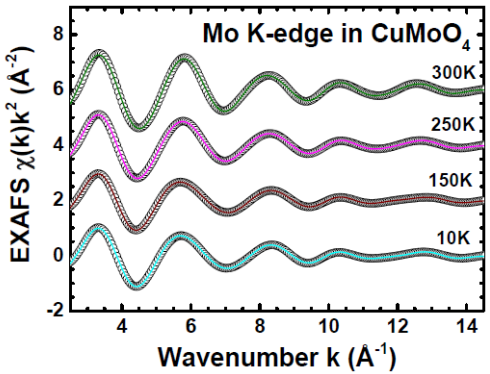

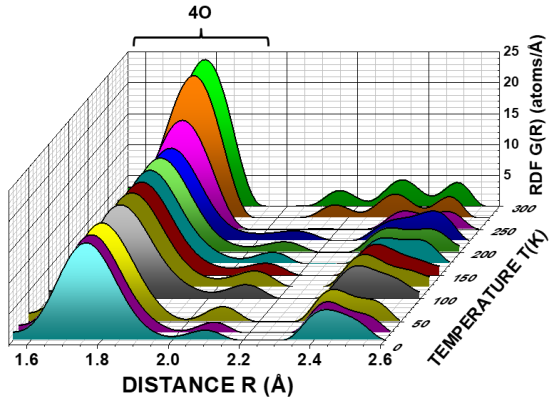

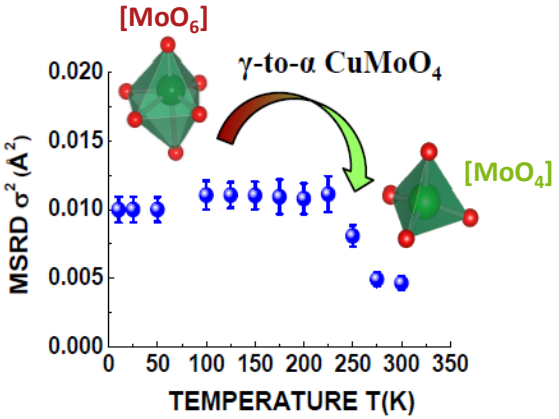

MSRD = mean-square relative displacement

$$\sigma^2 = \sigma^2_{static} + \sigma^2_{thermal}$$

Regularization based technique (EDARDF code)

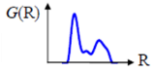

$$\chi_n(k) = S_0^2 \int_0^{+\infty} g_i(R) \frac{|f_i(k,R_i)|}{kR_i^2} e^{\frac{-2R_i}{\lambda(k)}} \sin(2kR_i + 2\delta(k) + \phi_i(k,R_i))dR$$

Regularization method: Yu.A. Babanov et al., Phys. Stat. Solidi (B) 105 (1981) 747.
EDARDF: A. Kuzmin, Physica B:Condensed Matter 208 (1995) 175-176.

γ → α phase transition occurs gradually, the molybdenum coordination by oxygen atoms changes from strongly distorted octahedral to less distorted tetrahedral.

I. Jonane, A. Cintins, A. Kalinko, R. Chernikov, A. Kuzmin, Phys. Status Solidi B 255 (2018) 1800074.

EXAFS DATA ANALYSIS

Reverse Monte Carlo modelling with evolutionary algorithm approach

EvAX code:
http://www.dragon.lv/evax/

1 Initial structure model

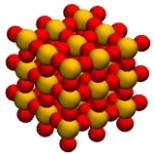

R.L. McGreevy and L. Pusztai, Mol. Simul. 1 (1988) 359-367.

J. Timoshenko, et al., J. Phys.: Condens. Matter 26 (2014) 055401.

2 Calculations of EXAFS data

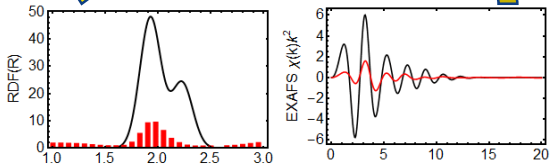

3 Testing agreement of theoretical data with experimental

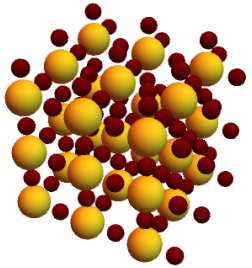

4 Random displacements of atoms (or some other update of 3D structure)

5 Analysis of final structure

N, R, σ^2

J.Timoshenko

EXAFS DATA ANALYSIS

Reverse Monte Carlo modelling with evolutionary algorithm approach

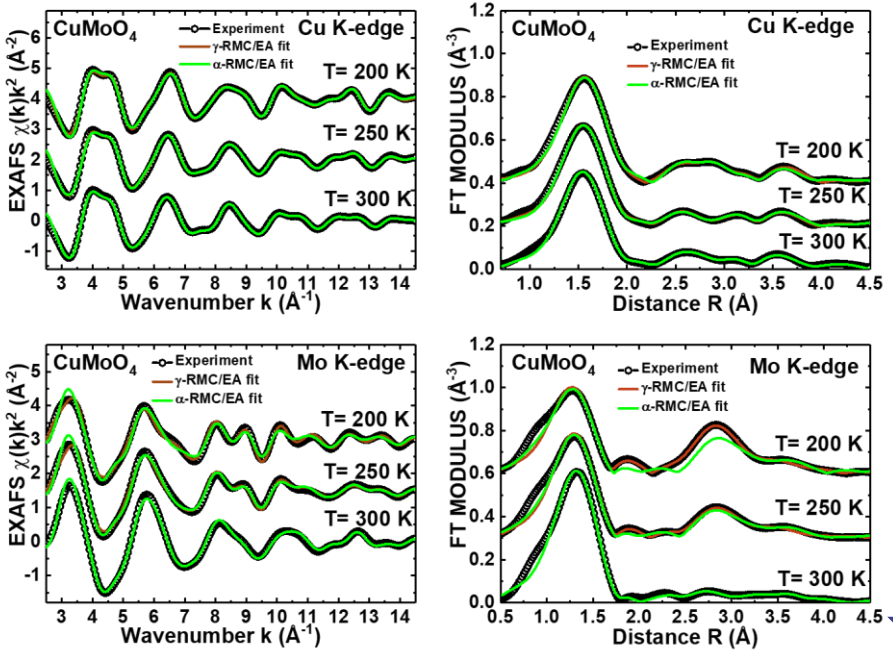

At T=250 K, two phases coexist.

EXAFS DATA ANALYSIS

Reverse Monte Carlo modelling with evolutionary algorithm approach

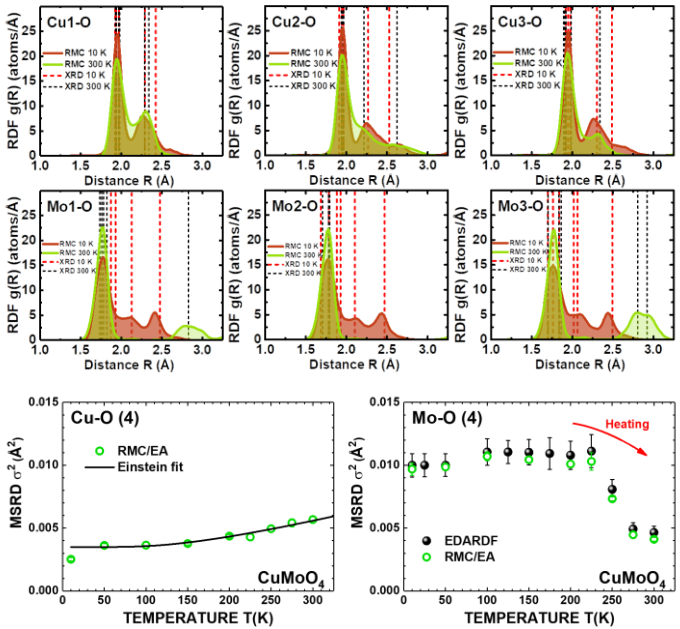

Information about the local environment around selected atoms.

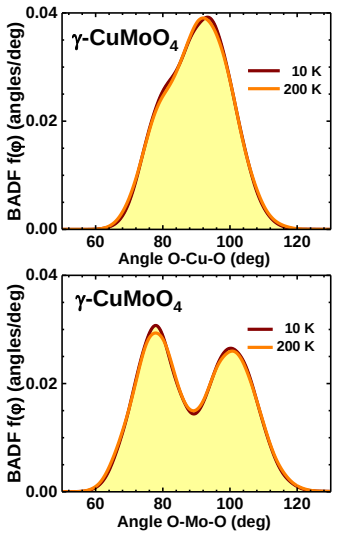

Different types of distortions of metal-oxygen octahedra reflected by BADFs.

RMC/EA modelling allows one to follow the variation of local environment in low-symmetry structures as $CuMoO_4$ on temperature.

I. Jonane, A. Cintins, A. Kalinko, R. Chernikov, A. Kuzmin, *Rad. Phys. Chem.* 175 (2020) 108112;

$CuMoO_4$ AT HIGH TEMPERATURES-XANES

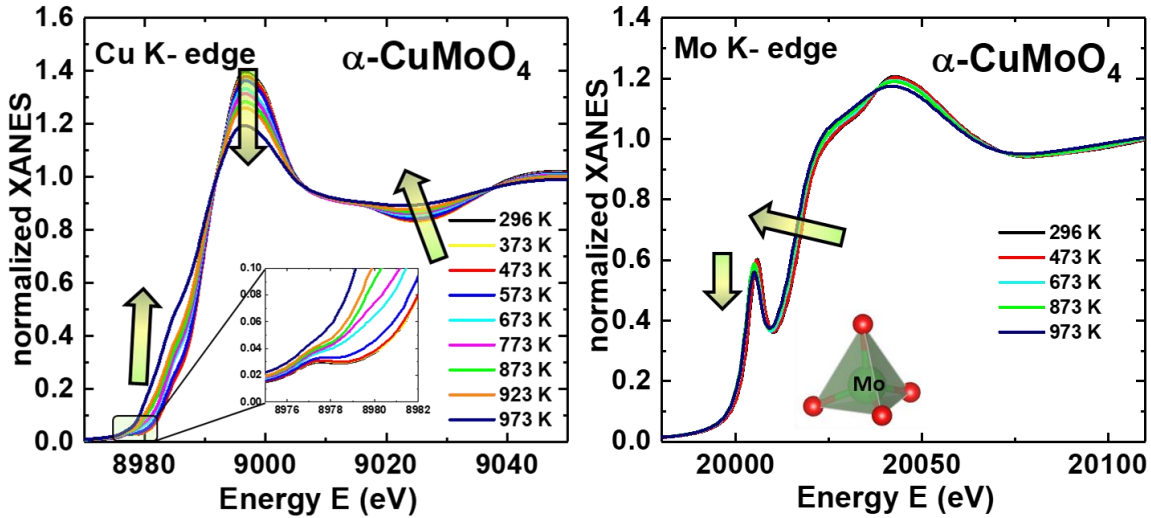

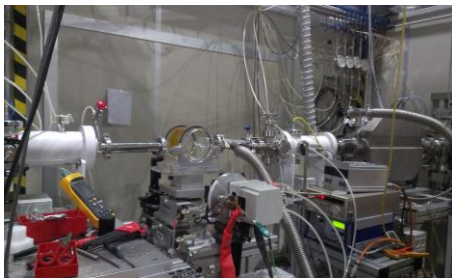

Rare temperature dependence of XANES region at the Cu K-edge is observed.

$$\chi_n(k) = S_0^2 \sum_i \frac{N_i |f_i(k,R_i)|}{kR_i^2} \sin(2kR_i + 2\delta(k) + \phi_i(k,R_i)) e^{\frac{-2R_i}{\lambda(k)}} e^{-2R_i k^2 \sigma_i^2}$$

$$k \to 0; e^{-2R_i k^2 \sigma_i^2} \to 1$$

I. Jonane, A. Anspoks, G. Aquilanti, A. Kuzmin, *Acta Mater.* 179 (2019) 26-35.

Temperature effect on XANES - examples

Mg K-edge

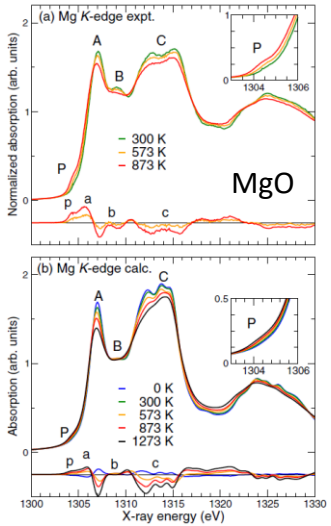

R. Nemausat et al. "**Phonon effects on x-ray absorption and nuclear magnetic resonance spectroscopies**" *Physical Review B* 92 (2015): 144310.

Al K-edge

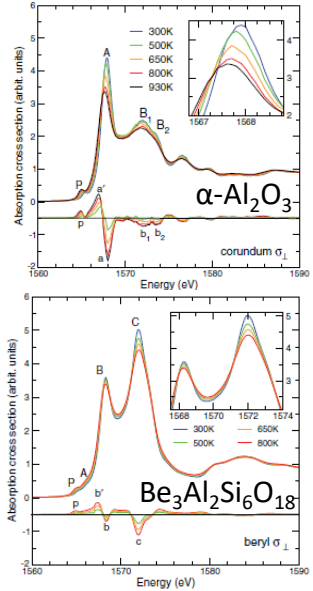

D. Manuel, et al. "**Experimental evidence of thermal fluctuations on the X-ray absorption near-edge structure at the aluminum K edge.**" *Physical Review B* 85 (2012) 224108.

Ti K-edge

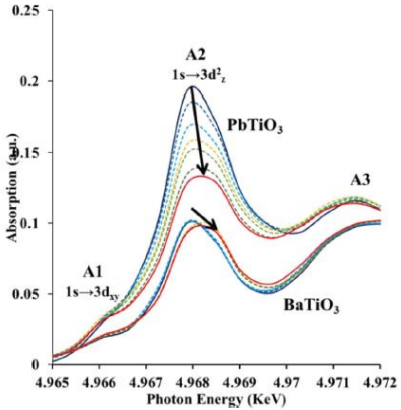

Figure 2. Temperature variation ($BaTiO_3$ 300–400 K and $PbTiO_3$ 500–800 K) of the pre-edge peaks in the Ti K-edge XANES spectra of tetragonal perovskite-type $BaTiO_3$ and $PbTiO_3$.

A Yoshiasa, et al. "**Determination of Ferro-and Antiferroelectricity Using the Temperature Dependence of the Pre-Edge Features in the XANES Spectra: XANES Study of Tetragonal and Cubic $ATiO_3$ (A= Sr, Ba, and Pb) and $PbZrO_3$**" Phys. Status Solidi B 255 (2018) 1800050.

THEORETICAL XANES CALCULATIONS

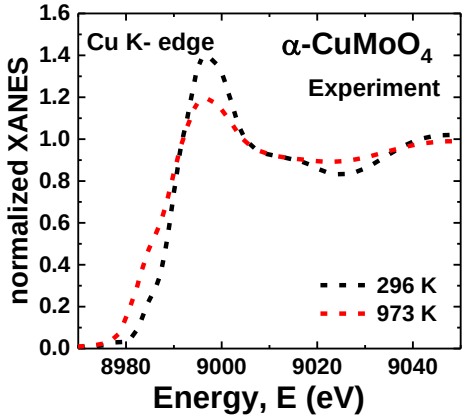

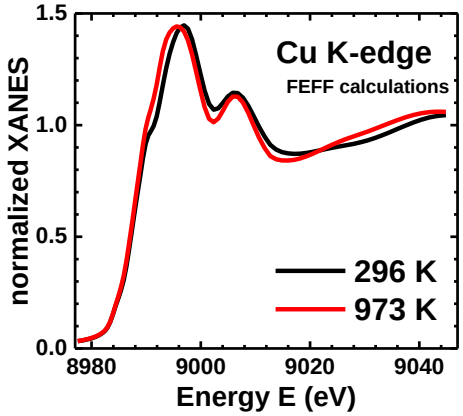

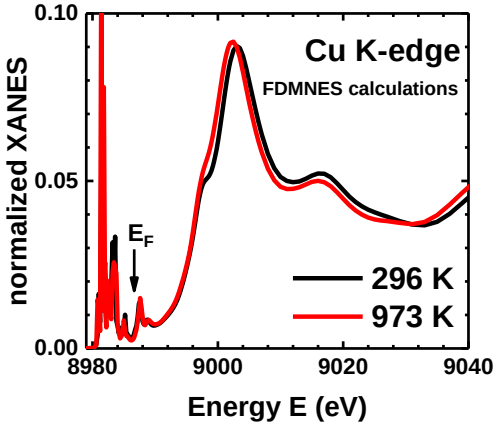

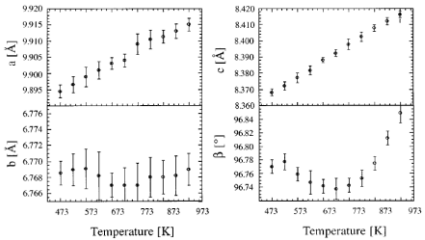

M. Wiesmann, et al., J. Solid State Chem. 132 (1997) 88-97.

The use of equilibrium atomic positions obtained from XRD does not allow one to obtain good agreement between the experimental and calculated XANES even when temperature dependence of the unit cell parameters is considered.

HOW TO ACCOUNT FOR TEMPERATURE IN XANES?

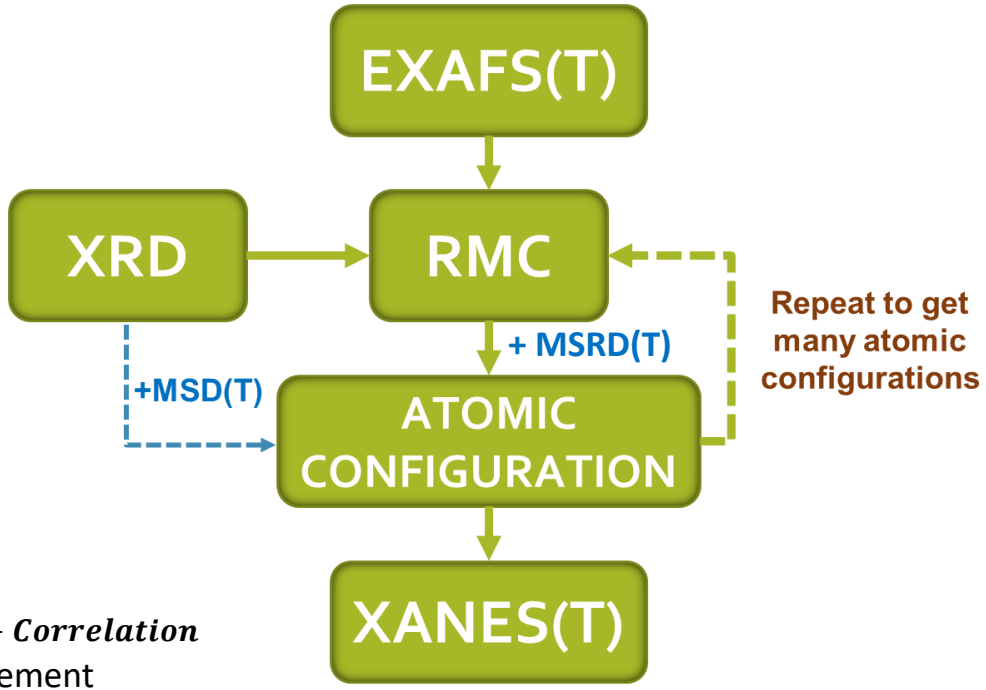

$$MSRD_{AB} = MSD_A + MSD_B - Correlation$$

MSD - mean-square displacement

MSRD - mean-square relative displacement

$CuMoO_4$ AT HIGH TEMPERATURES-EXAFS

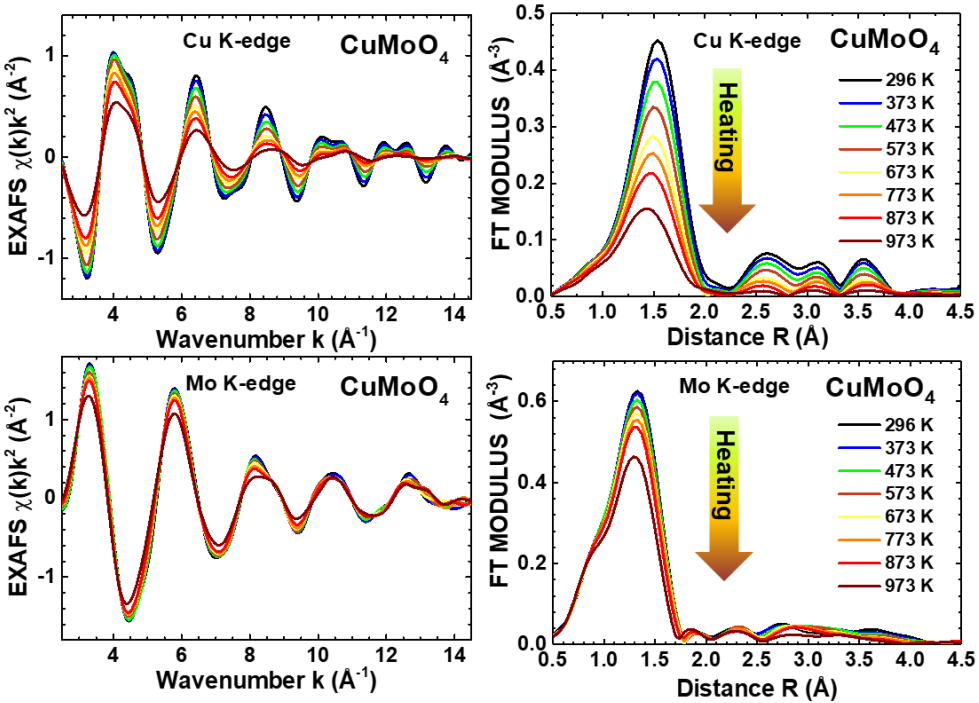

Always $[MoO_4]$!

$CuMoO_4$ AT HIGH TEMPERATURES

Reverse Monte Carlo modelling with evolutionary algorithm approach

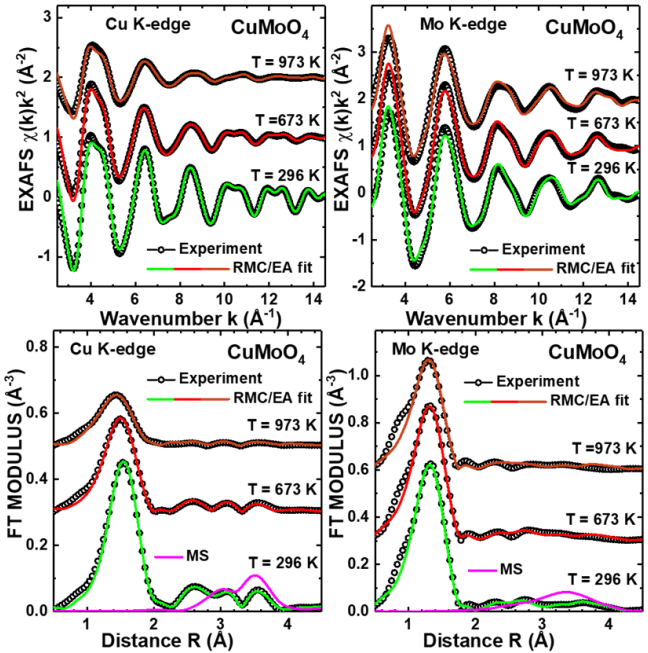

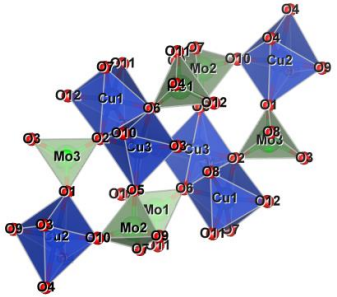

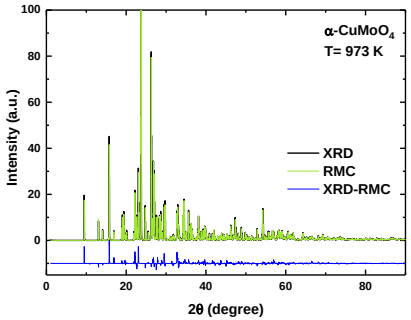

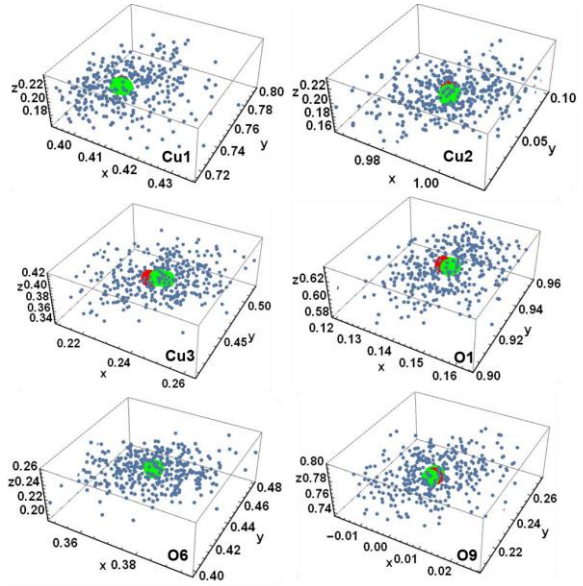

Average Wyckoff positions calculated for RMC structure models are close to those of XRD.

I. Jonane, A. Anspoks, G. Aquilanti, A. Kuzmin, *Acta Mater*. 179 (2019) 26-35.

$CuMoO_4$ AT HIGH TEMPERATURES-XANES RESULTS

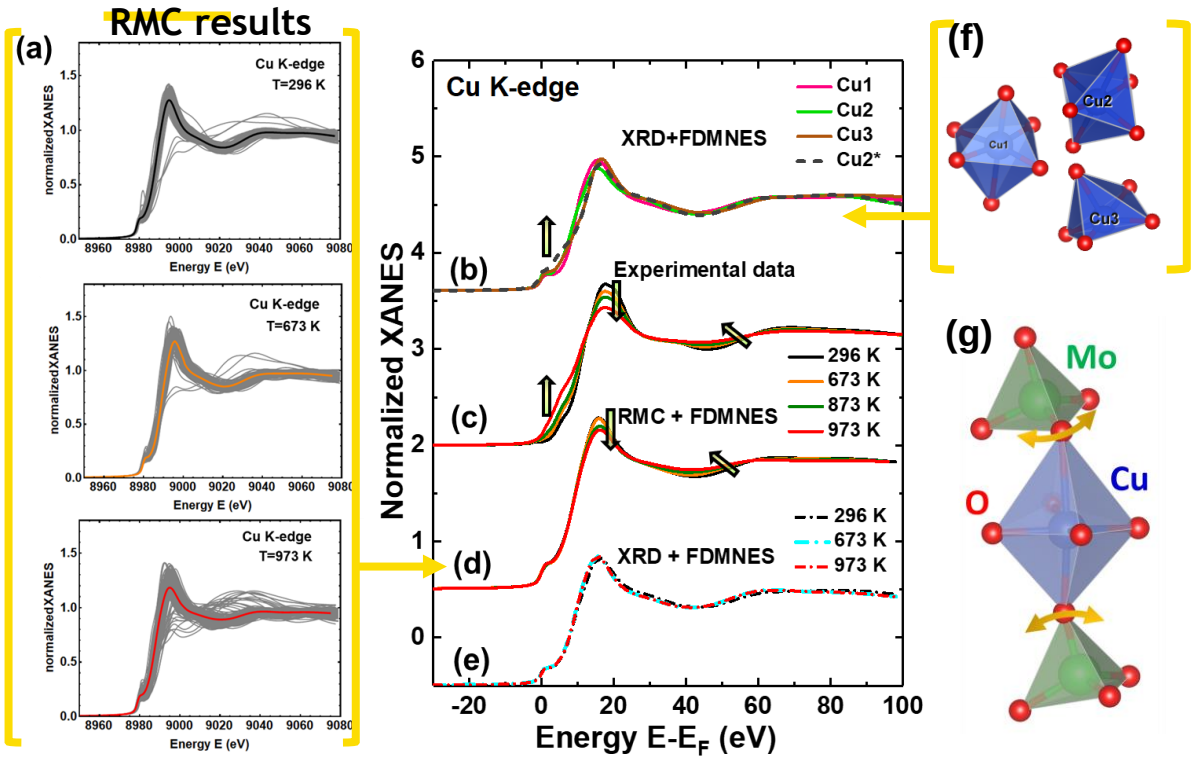

The simulated XANES spectra are in good agreement with the experiment and reproduce the main temperature dependence of XANES features.

The reduction of correlation in atomic motion between Cu and axial O atoms occurs upon temperature increase.

This dynamic effect is proposed to be the main cause for the temperature-induced changes in the $O^{2-} \rightarrow Cu^{2+}$ charge transfer processes.

I. Jonane, A. Anspoks, G. Aquilanti, A. Kuzmin, *Acta Mater*. 179 (2019) 26-35.

SUMMARY AND CONCLUSIONS

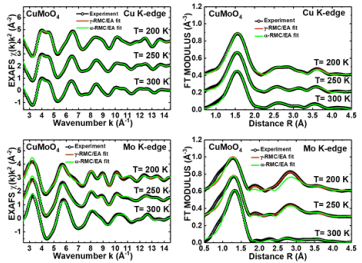

Data analysis of EXAFS spectra at the Cu and Mo K-edges simultaneously by RMC method, allows one to follow the temperature variation of the local environment in low symmetry materials as $CuMoO_4$.

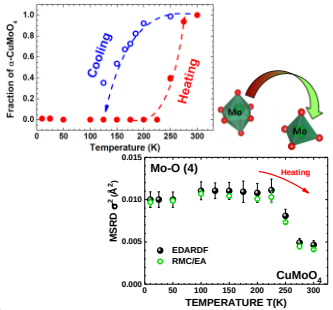

At low temperatures, γ→α phase transition occurs gradually, the molybdenum coordination by oxygen atoms changes from strongly distorted octahedral to less distorted tetrahedral.

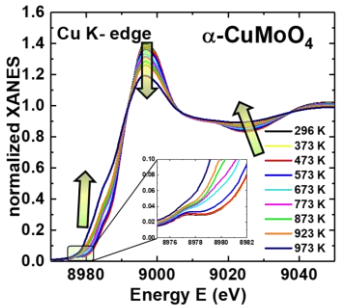

At high temperatures, experimental Cu K-edge X-ray absorption spectra show well pronounced temperature effect.

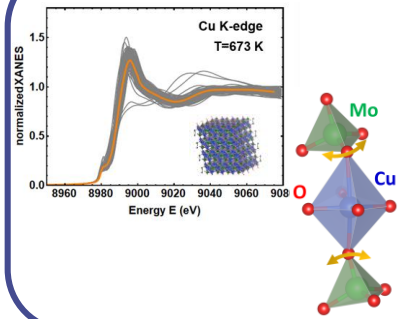

Structural models obtained by RMC were used to simulate the Cu K-edge XANES spectra to account for temperature effects.
The reduction of correlation in atomic motion between Cu and axial O atoms occurs upon temperature increase.

The financial support provided by the Latvian Council of Science project No. lzp-2019/1-0071 and L'ORÉAL Baltic "For Women In Science" Program with the support of the Latvian National Commission for UNESCO and the Latvian Academy of Sciences are greatly acknowledged.

THANK YOU

LATVIJAS UNIVERSITĀTES
CIETVIELU FIZIKAS INSTITŪTS

INSTITUTE OF SOLID STATE PHYSICS
UNIVERSITY OF LATVIA